

Gravitational wave signals in an Unruh-de Witt detector

Tomislav Prokopec[◇]

Institute for Theoretical Physics, Spinoza Institute & EMMEΦ
Utrecht University, Princetonplein 5, 3584 CC Utrecht, The Netherlands

Abstract

We firstly generalize the massive scalar propagator for gravitational waves propagating on Minkowski space obtained recently in Ref. [1]. We then use this propagator to study the response of a freely falling Unruh-de Witt detector to a gravitational wave background. We find that a freely falling detector completely cancels the effect of the deformation of the invariant distance induced by the gravitational waves, such that the only effect comes from an increased average size of scalar field vacuum fluctuations, the origin of which can be traced back to the change of the surface in which the gravitational waves fluctuate. When resummed over classical graviton insertions, gravitational waves generate cuts on the imaginary axis of the complex $\Delta\tau$ -plane (where $\Delta\tau = \tau - \tau'$ denotes the difference of proper times), and the discontinuity across these cuts is responsible for a continuum of energy transitions induced in the Unruh-de Witt detector. Not surprisingly, we find that the detector's transition rate is exponentially suppressed with increasing energy and the mass of the scalar field. What is surprising, however, is that the transition rate is *nonanalytic function* of the gravitational field strain. This means that, no matter how small is the gravitational field amplitude, expanding in powers of the gravitational field strain cannot approximate well the detector's transition rate. We present numerical and approximate analytical results for the detector's transition rate both for nonpolarized and for selected polarized monochromatic, unidirectional, gravitational waves.

[◇] e-mail: T.Prokopec@uu.nl

1 Introduction

In this work we calculate the response of a freely falling Unruh-de Witt detector which couples to massless or massive scalar field fluctuating in the presence of planar gravitational waves propagating on Minkowski spacetime. This work builds on earlier studies [2, 3, 4, 7, 8, 9, 1], which address some aspects of the problem of how planar gravitational waves affect scalar fields. In particular the authors of Ref. [9] investigate the response of freely-falling and accelerating Unruh-DeWitt detectors [10, 11, 12] in the presence of gravitational waves. In this work we generalize their analysis by using the propagator recently obtained in Ref. [1]. For simplicity, we do not analyse here the response of the detector moving along noninertial trajectories.

The model. In this work we consider a real, self-interacting scalar field $\phi(x)$ whose action and Lagrangian are,

$$S[\phi] = \int d^D x \sqrt{-g} \mathcal{L}_\phi, \quad \mathcal{L}_\phi = -\frac{1}{2}(\partial_\mu \phi)(\partial_\nu \phi)g^{\mu\nu} - \frac{m^2}{2}\phi^2 - \frac{\lambda}{4!}\phi^4, \quad (1.1)$$

where $g = \det[g_{\mu\nu}]$, $g^{\mu\nu}$ is the inverse of the metric tensor $g_{\mu\nu}$, m is the field's mass and λ is the self-interaction coupling strength. We work in natural units in which $c = 1$, but keep the dependence on \hbar explicit. This means that the dimension of the field ϕ and the mass m is m^{-1} , and λ is dimensionless. To restore the physical dimension of m , one ought to rescale it as, $m \rightarrow mc/\hbar$.

1.1 Gravitational waves

We are interested in understanding the effects of gravitational waves on scalar fields. A convenient representation for a gravitational wave background is,

$$g_{\mu\nu}(x) = \eta_{\mu\nu} + h_{\mu\nu}(x), \quad (1.2)$$

where $h_{\mu\nu}(x)$ is a perturbation of the metric tensor $g_{\mu\nu}$ around flat Minkowski space, characterised by Minkowski metric $\eta_{\mu\nu}$, which is in Cartesian coordinates a $D \times D$ diagonal matrix of the form, $\eta_{\mu\nu} = \text{diag}(-1, 1, 1, \dots)$. In the traceless-transverse gauge (in which the gravitational field perturbation $h_{\mu\nu}$ is gauge invariant to linear order in the gravitational field), planar gravitational waves moving in the x^{D-1} direction ($x^{D-1} \rightarrow z$ when $D = 4$) satisfy $h_{0\mu} = 0$ and

$$h_{ij}(u) = \begin{pmatrix} h_{xx}(u) & h_{xy}(u) & \cdots & h_{xD-2}(u) & 0 \\ h_{xy}(u) & h_{yy}(u) & \cdots & h_{yD-2}(u) & 0 \\ \vdots & \vdots & \vdots & \cdots & \vdots \\ h_{xD-2}(u) & h_{yD-2}(u) & \cdots & h_{D-2D-2}(u) & 0 \\ 0 & 0 & \cdots & 0 & 0 \end{pmatrix}, \quad (1.3)$$

where $u = t - x^{D-1}$ is a lightcone coordinate. Note that some of the elements of h_{ij} in Eq. (1.3) may vanish. In $D = 4$ dimensions this simplifies to planar gravitational waves with nonvanishing elements in the xy -plane. In practical calculations it is often convenient to simplify (1.3) by assuming that nonvanishing elements of h_{ij} are in the upper left 2×2 block.

In this work we generalize the monochromatic wave background considered in Ref. [1] to the case when the gravitational wave strain, $h_{ij} = h_{ij}(u)$, is characterised by a general function of u propagating in the x^{D-1} direction. Motivated by the form of gravitational waves emitted by realistic sources, whose

wave form can be decomposed into the fundamental mode of frequency ω_g , and the higher overtones (whose frequencies are $n\omega_g$), we shall consider gravitational waves of the form,

$$h_{ij}(u) = \sum_{n=1}^{\infty} h_{ij}^{(n)} \cos(n\omega_g u + \psi_{ij}^{(n)}), \quad (1.4)$$

where $h_{ij}^{(n)}$ and $\psi_{ij}^{(n)}$ are the (time independent) gravitational field amplitudes and phases of the n -th harmonic. Such gravitational waves are formed by binary systems whose components harbor angular momentum and/or strong magnetic fields [13, 14]. It is important to keep in mind that, even when gravitational waves are nonpolarized, the perceived amplitudes of the $+$ and \times polarizations will differ, unless the source is *face on*, *i.e.* the inclination angle is zero. This means that the only fixed characteristic of nonpolarized gravitational waves is the relative phase difference, $\Delta\psi = \psi_+ - \psi_\times = \pm\pi/2$.

The gravitational waves considered here have a phase velocity, $\vec{v}_{\text{ph}} = \hat{z}$, and are often referred to as the positive frequency solutions. In addition there are negative frequency gravitational waves, with an opposite phase velocity ($\vec{v}_{\text{ph}} = -\hat{z}$), for which $h_{ij} = h_{ij}(v)$, with $v = t + z$ ($v = t + x^{D-1}$ in the D dimensional case). Sufficiently close to the gravitational wave source the gravitational wave propagates radially, such that in a relatively small spatial volume one can approximate the wave by $h_{ij}(u)$.

2 Scalar propagator

Variation of the action (1.1) gives a Klein-Gordon equation satisfied by the scalar field operator $\hat{\phi}(x)$,

$$(\square - m^2)\hat{\phi}(x) = 0, \quad (2.1)$$

where $\square = \frac{1}{\sqrt{-g}}\partial_\mu\sqrt{-g}g^{\mu\nu}\partial_\nu$ is the d'Alembertian operator as it acts on a scalar field, and we have neglected in Eq. (2.1) the quartic selfcoupling. The positive and negative frequency Wightman functions are defined as the following two-point functions,

$$i\Delta^{(+)}(x; x') = \langle \Omega | \hat{\phi}(x)\hat{\phi}(x') | \Omega \rangle, \quad (2.2)$$

$$i\Delta^{(-)}(x; x') = \langle \Omega | \hat{\phi}(x')\hat{\phi}(x) | \Omega \rangle, \quad (2.3)$$

where $|\Omega\rangle$ denotes a state of the scalar field, which for simplicity we choose to be the vacuum state. When the field operator in Eq. (2.1) is expanded in terms of the momentum space mode functions, one can reduce the problem of obtaining the Wightman functions to performing the momentum integrals in Eqs. (5.1–5.2) over products of the mode functions. These integrals can be performed by a straightforward generalization of the method presented in Appendices A and B of Ref. [1] (see also Appendix A of this work), resulting in,

$$i\Delta^{(\pm)}(x; x') = \frac{\hbar m^{D-2}}{(2\pi)^{\frac{D}{2}} [\gamma(u)\gamma(u')]^{\frac{1}{4}} \sqrt{\Upsilon(u; u')}} \frac{K_{\frac{D-2}{2}}(m\sqrt{\Delta\bar{x}_{(\pm)}^2})}{(m\sqrt{\Delta\bar{x}_{(\pm)}^2})^{\frac{D-2}{2}}}, \quad (2.4)$$

where $K_\nu(z)$ denotes Bessel's function of the second kind, and $\Delta\bar{x}_{(\pm)}^2(x; x')$ are the deformed distance functions (that violate global Lorentz symmetry), which in lightcone coordinates can be written as,

$$\Delta\bar{x}_{(\pm)}^2(x; x') = -(\Delta u \mp i\epsilon)(\Delta v \mp i\epsilon) + \begin{pmatrix} \Delta x & & & \\ \Delta y & & & \\ \vdots & & & \\ \Delta x^{D-2} & & & \end{pmatrix} \cdot \mathcal{G}(u; u'), \quad (2.5)$$

and in Cartesian coordinates,

$$\Delta \bar{x}_{(\pm)}^2(x; x') = -(\Delta t \mp i\epsilon)^2 + \begin{pmatrix} \Delta x & \Delta y & \cdots & \Delta x^{D-2} \end{pmatrix} \cdot \mathcal{G}(u; u') \cdot \begin{pmatrix} \Delta x \\ \Delta y \\ \vdots \\ \Delta x^{D-2} \end{pmatrix} + \Delta x_{D-1}^2, \quad (2.6)$$

where $\Delta x^\mu = x^\mu - x'^\mu$. This global Lorentz violation is mediated by the (symmetric) deformation matrix,

$$\mathcal{G}(u; u') = \begin{pmatrix} \mathcal{G}_{xx}(u; u') & \mathcal{G}_{xy}(u; u') & \cdots & \mathcal{G}_{xD-2}(u; u') \\ \mathcal{G}_{xy}(u; u') & \mathcal{G}_{yy}(u; u') & \cdots & \mathcal{G}_{yD-2}(u; u') \\ \vdots & \vdots & \vdots & \vdots \\ \mathcal{G}_{xD-2}(u; u') & \mathcal{G}_{yD-2}(u; u') & \cdots & \mathcal{G}_{yD-2}(u; u') \end{pmatrix}, \quad (2.7)$$

which is the inverse of the corresponding momentum space deformation matrix $\Upsilon(u; u')$, $\mathcal{G}(u; u') = \Upsilon^{-1}(u; u')$. The general form of Υ is,

$$\Upsilon(u; u') = \frac{1}{\Delta u} \left[\int^u d\bar{u} \begin{pmatrix} g^{xx}(\bar{u}) & g^{xy}(\bar{u}) & \cdots & g^{xD-2}(\bar{u}) \\ g^{xy}(\bar{u}) & g^{yy}(\bar{u}) & \cdots & g^{yD-2}(\bar{u}) \\ \vdots & \vdots & \vdots & \vdots \\ g^{xD-2}(\bar{u}) & g^{yD-2}(\bar{u}) & \cdots & g^{D-2D-2}(\bar{u}) \end{pmatrix} - (u \rightarrow u') \right], \quad (2.8)$$

where $g^{ij}(u)$ denote the inverse of $g_{ij}(u)$. For example, for gravitational waves oscillating in the xy plane, only the distances in this plane (which we denote by \perp) get deformed, such that the nontrivial elements of the deformation matrix are,

$$\begin{aligned} \Upsilon^\perp(u; u') &= \frac{1}{\Delta u} \left[\int^u d\bar{u} \begin{pmatrix} g^{xx}(\bar{u}) & g^{xy}(\bar{u}) \\ g^{xy}(\bar{u}) & g^{yy}(\bar{u}) \end{pmatrix} - (u \rightarrow u') \right] \\ &= \frac{1}{\Delta u} \left[\int^u \frac{d\bar{u}}{\gamma(\bar{u})} \begin{pmatrix} g_{yy}(\bar{u}) & -g_{xy}(\bar{u}) \\ -g_{xy}(\bar{u}) & g_{xx}(\bar{u}) \end{pmatrix} - (u \rightarrow u') \right], \end{aligned} \quad (2.9)$$

where $\gamma(u) = \det[g_{ij}(u)]$. For monochromatic non-polarized gravitational waves in linear representation one obtains (see section 3 of Ref. [1] for more details),

$$\mathcal{G}^\perp(u; u') = \frac{1}{\gamma \Upsilon(u; u')} \begin{pmatrix} 1 + h \frac{\sin(\omega_g u) - \sin(\omega_g u')}{\omega_g \Delta u} & -h \frac{\cos(\omega_g u) - \cos(\omega_g u')}{\omega_g \Delta u} \\ -h \frac{\cos(\omega_g u) - \cos(\omega_g u')}{\omega_g \Delta u} & 1 - h \frac{\sin(\omega_g u) - \sin(\omega_g u')}{\omega_g \Delta u} \end{pmatrix}, \quad (2.10)$$

$$\Upsilon(u; u') \equiv \det[\Upsilon] = \det[\Upsilon^\perp] = \frac{1}{\gamma^2} \left[1 - h^2 j_0^2\left(\frac{\omega_g \Delta u}{2}\right) \right], \quad (2.11)$$

where $j_0(z) = \sin(z)/z$ is the spherical Bessel function, $\gamma(u) = 1 - h^2$ is time independent, $h = h_+ = h_\times$, and $h_+ = h_{xx} = -h_{yy}$ and $h_\times = h_{xy}$ are the amplitudes of the two polarizations. The matrix $\mathcal{G}^\perp(u; u')$ deforms distances in position space according to Eqs. (2.5–2.6).

On the other hand, for polarized monochromatic waves fluctuating in the xy -plane one obtains for the (+)-polarized waves ($h_+ \neq 0$, $h_\times = 0$),

$$\Upsilon^\perp = \frac{2}{\omega_g \Delta u} \frac{1}{\sqrt{1 - h_+^2}} \left\{ \begin{pmatrix} \arctan \left[\sqrt{\frac{1 - h_+}{1 + h_+}} \tan\left(\frac{\omega_g u}{2}\right) \right] & 0 \\ 0 & \arctan \left[\sqrt{\frac{1 + h_+}{1 - h_+}} \tan\left(\frac{\omega_g u}{2}\right) \right] \end{pmatrix} - (u \rightarrow u') \right\}, \quad (2.12)$$

and for the (\times)-polarized waves ($h_+ = 0$, $h_\times \neq 0$),

$$\mathbf{r}^\perp = \frac{1}{\omega_g \Delta u} \frac{1}{\sqrt{1-h_\times^2}} \left\{ \left(\begin{array}{cc} \arctan \left[\frac{1}{\sqrt{1-h_\times^2}} \tan(\omega_g u) \right] & -\arctan \left[\frac{h_\times}{\sqrt{1-h_\times^2}} \sin(\omega_g u) \right] \\ -\arctan \left[\frac{h_\times}{\sqrt{1-h_\times^2}} \sin(\omega_g u) \right] & \arctan \left[\frac{1}{\sqrt{1-h_\times^2}} \tan(\omega_g u) \right] \end{array} \right) - (u \rightarrow u') \right\}, \quad (2.13)$$

respectively.

From the Wightman functions (2.4) one can easily construct the Feynman propagator. In lightcone coordinates we have,

$$\begin{aligned} i\Delta_{F,LC}(x; x') &\equiv \Theta(\Delta u) i\Delta^{(+)}(x; x') + \Theta(-\Delta u) i\Delta^{(-)}(x; x') \\ &= \frac{\hbar m^{D-2}}{(2\pi)^{\frac{D}{2}} [\gamma(u)\gamma(u')]^{\frac{1}{4}} \sqrt{\Upsilon(u; u')}} \frac{K_{\frac{D-2}{2}}(m\sqrt{\Delta\bar{x}_{F,LC}^2})}{(m\sqrt{\Delta\bar{x}_{F,LC}^2})^{\frac{D-2}{2}}}, \end{aligned} \quad (2.14)$$

and in Cartesian coordinates,

$$\begin{aligned} i\Delta_F(x; x') &\equiv \Theta(\Delta t) i\Delta^{(+)}(x; x') + \Theta(-\Delta t) i\Delta^{(-)}(x; x') \\ &= \frac{\hbar m^{D-2}}{(2\pi)^{\frac{D}{2}} [\gamma(u)\gamma(u')]^{\frac{1}{4}} \sqrt{\Upsilon(u; u')}} \frac{K_{\frac{D-2}{2}}(m\sqrt{\Delta\bar{x}_F^2})}{(m\sqrt{\Delta\bar{x}_F^2})^{\frac{D-2}{2}}}. \end{aligned} \quad (2.15)$$

Both propagators (2.14–2.15) are suitable for perturbative studies, the former for the initial value problem defined on an $u = \text{constant}$ hypersurface, the latter on a $t = \text{constant}$ hypersurface. However, the two $i\epsilon$ prescriptions differ,

$$\begin{aligned} \Delta\bar{x}_{F,LC}^2(x; x') &= -(|\Delta u| - i\epsilon)(\pm\Delta v - i\epsilon) + \|\Delta\vec{x}_\perp\|^2, \\ \Delta\bar{x}_F^2(x; x') &= -(|\Delta t| - i\epsilon)^2 + \|\Delta\vec{x}\|^2. \end{aligned} \quad (2.16)$$

That means that the imaginary parts of the propagators differ. Both prescriptions are legitimate, as they are designated to study inequivalent perturbative evolution problems.

From Eqs. (2.14–2.15) one easily obtains the corresponding Dyson propagators,

$$i\Delta_{D,LC}(x; x') = [i\Delta_{F,LC}(x; x')]^*, \quad i\Delta_D(x; x') = [i\Delta_F(x; x')]^*, \quad (2.17)$$

which are important for studying time evolution of Hermitian operators in interacting quantum field theories.

One-loop results. In what follows we briefly summarize the one-loop calculations from Ref. [1] for the generalized gravitational waves of the form (1.3)

For the one-loop effective action calculation and one-loop scalar mass induced by the scalar self-interaction, one needs the coincident propagator (2.14–2.15), which is of the same form as in Eq. (4.4) of Ref. [1],

$$i\Delta_F(x; x) = \frac{\hbar m^{D-2}}{(4\pi)^{D/2} \sqrt{\gamma(u)\Upsilon(u; u)}} \Gamma\left(1 - \frac{D}{2}\right), \quad (2.18)$$

where $\gamma(u) = \det[g_{ij}]$ and $\Upsilon(u; u)$ is the determinant of the Υ matrix in Eq. (2.8) evaluated at spacetime coincidence. Applying the l'Hospital rule to Eq. (2.9) yields,

$$\Upsilon(u; u) = \begin{pmatrix} g^{xx}(u) & g^{xy}(u) & \cdots & g^{xD-2}(u) \\ g^{xy}(u) & g^{yy}(u) & \cdots & g^{yD-2}(u) \\ \vdots & \vdots & \ddots & \vdots \\ g^{xD-2}(u) & g^{yD-2}(u) & \cdots & g^{D-2D-2}(u) \end{pmatrix} \equiv g^{ij}(u), \quad (2.19)$$

from which it immediately follows that, $\Upsilon(u; u) = \det[\Upsilon(u; u)] = \det[g^{ij}(u)] = 1/\gamma(u)$, and therefore,

$$\gamma(u)\Upsilon(u; u) = 1. \quad (2.20)$$

This shows that both, the one-loop effective action and the one-loop scalar mass reduce to that of Minkowski space in Eqs. (4.12) and (4.15) of Ref. [1].

The calculation of the one-loop energy momentum tensor is more involved, but the procedure is the same as for the polarized gravitational waves in linear representation in section 5 of Ref. [1], and the resulting renormalized energy momentum tensor is identical in form as in Eqs. (5.29-5.30) of Ref. [1],

$$\langle \Omega | T^*[\hat{T}_{\mu\nu}^{\text{ren}}(x)] | \Omega \rangle = -\frac{\hbar m^4}{64\pi^2} \left[\ln\left(\frac{m^2}{4\pi\mu^2}\right) + \gamma_E - \frac{3}{2} \right] g_{\mu\nu}(u) - \frac{\hbar m^2}{96\pi^2} \left[\log\left(\frac{m^2}{4\pi\mu^2}\right) + \gamma_E - 1 \right] G_{\mu\nu}(u), \quad (2.21)$$

where $G_{\mu\nu}(u)$ is the classical Einstein tensor associated with the metric in Eqs. (1.2–1.3). The counterterms needed to renormalize (2.21) are generated by the cosmological constant action and the Hilbert-Einstein action, as detailed in Ref. [1].

3 Unruh-de Witt detector

In this section we study the response of a freely falling Unruh-de Witt detector [10, 11, 12] moving in the background of gravitational waves which propagate in the z -direction. This work generalizes the analysis of Ref. [9].

Freely falling observers. The line element for the problem at hand can be written from Eq. (1.2) as,

$$ds^2 = -dt^2 + dx^i g_{ij}(u) dx^j = -dudv + dx^i g_{ij}^\perp(u) dx^j, \quad (3.1)$$

where $g_{ij}^\perp(u)$ is a $(D-2) \times (D-2)$ dimensional symmetric metric tensor (in $D=4$ it reduces to a 2×2 dimensional symmetric metric). Useful killing vectors are, $K_v = \partial_v$ and $K_i = \partial_i$ ($i = 1, 2, \dots, D-2$), from which one obtains the corresponding conserved momenta,¹

$$P_v = -(K_v)_\mu \frac{dx^\mu}{d\tau} = \frac{1}{2} \frac{du}{d\tau}, \quad P_i = (K_i)_j \frac{dx^j}{d\tau} = g_{ij}^\perp(u) \frac{dx^j}{d\tau}, \quad (i, j = 1, 2, \dots, D-2), \quad (3.2)$$

where (for a later convenience) we chose the geodesic time $\lambda = \tau$ to be the proper time τ , defined by $d\tau^2 = -ds^2$. Upon inserting these equations into the line element (3.1) and dividing by $-d\tau^2$ one obtains,

$$1 = \frac{du}{d\tau} \frac{dv}{d\tau} - \frac{dx^i}{d\tau} g_{ij}^\perp(u) \frac{dx^j}{d\tau} = 2P_v \frac{dv}{d\tau} - P_i g_{ij}^\perp(u) P_j. \quad (3.3)$$

¹Recall that each Killing vector K obeys a Killing equation, $\nabla_{(\mu} K_{\nu)} = 0$, and generates a conserved quantity, $P = K_\mu \frac{dx^\mu}{d\lambda}$.

This generates the geodesic equation for $dv/d\tau$,

$$\frac{dv}{d\tau} = \frac{1}{2P_v} \left(1 + P_i g_{\perp}^{ij}(u) P_j \right), \quad (3.4)$$

whose formal solution is,

$$v(\tau) = v_0 + \frac{1}{2P_v} \left(\tau + \frac{P_i}{2P_v} \int_{u_0}^u d\bar{u} g_{\perp}^{ij}(\bar{u}) P_j \right), \quad (v_0 \equiv v(0), u_0 \equiv u(0)), \quad (3.5)$$

where we made use of, $du/d\tau = 2P_v$. Next, one can solve equations (3.2) to obtain,

$$u(\tau) = u_0 + 2P_v \tau, \quad (u_0 \equiv u(0)) \quad (3.6)$$

$$x^i(\tau) = x_0^i + \frac{1}{2P_v} \int_{u_0}^u d\bar{u} g_{\perp}^{ij}(\bar{u}) P_j, \quad (x_0^i \equiv x^i(0)), \quad (3.7)$$

such that Eq. (3.5) can be also written as,

$$v(\tau) = v_0 + \frac{1}{2P_v} \left(\tau + P_i (x^i(u) - x_0^i) \right). \quad (3.8)$$

From Eq. (3.6) we see that one can always replace τ with u ,

$$\tau(u) = \frac{u - u_0}{2P_v}. \quad (3.9)$$

Unruh-de Witt detector. An Unruh-de Witt detector [10, 11, 12] is a detector with a monopolar coupling to a scalar field ϕ , which can be represented by the interaction Lagrangian,

$$\mathcal{L}_{\text{int}} = -gm(t)\phi(x), \quad (3.10)$$

where $m(t)$ is the monopole moment of the detector and g a coupling constant. At the first order of perturbation theory, the transition amplitude from the ground state, $|E_0\rangle \otimes |\Omega\rangle$ (where $|E_0\rangle$ denotes the ground state of the detector with energy E_0 and $|\Omega\rangle$ denotes the ground state of the scalar field) to a state $|E\rangle \otimes |\Psi\rangle$ (where $|E\rangle$ is an excited state of the detector with energy $E > E_0$), is given by,

$$\mathcal{A}(E_0 \rightarrow E) = ig \int_{-\infty}^{\infty} \langle E | \hat{m}(\tau) | E_0 \rangle \langle \Psi | \hat{\phi}(x(\tau)) d\tau | \Omega \rangle, \quad (3.11)$$

where τ is the geodesic time and $x^\mu(\tau)$ parametrises a geodesic. The probability P that the detector transits from E_0 to E is obtained by squaring the transition amplitude, and summing over all intermediate (excited) states of the field $|\Psi\rangle$, resulting in,

$$P = g^2 \sum_E |\langle E | \hat{m}(0) | E_0 \rangle|^2 \mathcal{F}(\Delta E), \quad (3.12)$$

where we made use of, $\hat{m}(0) = e^{-i\hat{H}_0\tau} \hat{m}(\tau) e^{i\hat{H}_0\tau}$, denoting the monopole moment evolved back to the initial time $\tau = 0$, and $\mathcal{F}(\Delta E)$ denotes the response function of the detector given by,

$$\mathcal{F}(\Delta E) = \int_{-\infty}^{\infty} d\tau \int_{-\infty}^{\infty} d\tau' e^{-i\Delta E(\tau-\tau')} i\Delta^{(+)}(x^\mu(\tau); x^\nu(\tau')), \quad \Delta E = E - E_0. \quad (3.13)$$

Here $i\Delta^{(+)}(x^\mu(\tau); x^\nu(\tau'))$ is the positive frequency Wightman function (2.4) evaluated along the geodesics of the detector,

$$x^\mu = x^\mu(\tau), \quad x^\nu = x^\nu(\tau'). \quad (3.14)$$

It is useful to transform the integrals in Eq. (3.13) to the relative and average proper times, $\Delta\tau = \tau - \tau'$ and $T = (\tau + \tau')/2$,

$$\mathcal{F}(\Delta E) = \int_{-\infty}^{\infty} dT \int_{-\infty}^{\infty} d\Delta\tau e^{-i\Delta E\Delta\tau} i\Delta^{(+)}(x^\mu(T + \Delta\tau/2); x^\nu(T - \Delta\tau/2)), \quad (3.15)$$

such that one can define the *transition rate* \mathcal{R} as the rate of detector's transitions, $E_0 \rightarrow E$, per unit time,

$$\begin{aligned} \mathcal{R}(T, \Delta E) &= \lim_{\Delta T \rightarrow 0} \left[\frac{\Delta\mathcal{F}(\Delta E)}{\Delta T} \right] \\ &= \int_{-\infty}^{\infty} d\Delta\tau e^{-i\Delta E\Delta\tau} i\Delta^{(+)}(x^\mu(T + \Delta\tau/2); x^\nu(T - \Delta\tau/2)). \end{aligned} \quad (3.16)$$

By making use of the properties of the Wightman functions, $i\Delta^{(\pm)}(x; x') = i\Delta^{(\mp)}(x'; x) = [i\Delta^{(\pm)}(x'; x)]^*$, this can be rewritten as,

$$\begin{aligned} \mathcal{R}(T, \Delta E) &= \frac{1}{2} \int_{-\infty}^{\infty} d\Delta\tau \left\{ e^{-i\Delta E\Delta\tau} i\Delta^{(+)}(x^\mu(T + \Delta\tau/2); x^\nu(T - \Delta\tau/2)) \right. \\ &\quad \left. + e^{i\Delta E\Delta\tau} [i\Delta^{(+)}(x^\mu(T + \Delta\tau/2); x^\nu(T - \Delta\tau/2))]^* \right\} \end{aligned} \quad (3.17)$$

$$\begin{aligned} &= \int_0^{\infty} d\Delta\tau \left\{ e^{-i\Delta E\Delta\tau} i\Delta^{(+)}(x^\mu(T + \Delta\tau/2); x^\nu(T - \Delta\tau/2)) \right. \\ &\quad \left. + e^{i\Delta E\Delta\tau} [i\Delta^{(+)}(x^\mu(T + \Delta\tau/2); x^\nu(T - \Delta\tau/2))]^* \right\} \end{aligned} \quad (3.18)$$

$$= 2\Re \left[\int_0^{\infty} d\Delta\tau e^{-i\Delta E\Delta\tau} i\Delta^{(+)}(x^\mu(T + \Delta\tau/2); x^\nu(T - \Delta\tau/2)) \right], \quad (3.19)$$

where we made use of the invariance of the integral measure under, $\Delta\tau \rightarrow -\Delta\tau$, *i.e.* $\int_{-\infty}^{\infty} d\Delta\tau = \int_{-\infty}^{\infty} d(-\Delta\tau)$.

Now, from Eqs. (3.6–3.7) and (3.8) one easily obtains,

$$\Delta u(\tau) = 2P_v \Delta\tau, \quad (\Delta u_0 = 0), \quad (3.20)$$

$$\Delta x^i(\tau) = \frac{\Delta u}{2P_v} \mathcal{G}^{ij}(u; u') P_j, \quad (i, j = 1, 2, \dots, D-2, \Delta x_0^i = 0), \quad (3.21)$$

$$\Delta v = \frac{\Delta u}{4P_v^2} \left[1 + P_i \mathcal{G}^{ij}(u; u') P_j \right], \quad (\Delta v_0 = 0), \quad (3.22)$$

where $\Delta x_0^\mu = 0$ follows from the fact that we are considering worldlines of a single particle. From Eq. (3.20) we see that the conserved momentum $2P_v$ converts a proper time interval $\Delta\tau$ into the coordinate time interval Δu . When these are inserted into Eqs. (2.5) one obtains,

$$\begin{aligned} \Delta \bar{x}_{(\pm)}^2(x; x') &= -(\Delta u \mp i\epsilon) \left[\frac{\Delta u}{4P_v^2} (1 + P_i \mathcal{G}^{ij}(u; u') P_j) \mp i\epsilon \right] \\ &\quad + \left(\frac{\Delta u}{2P_v} \mathcal{G}^{ik}(u; u') P_k \right) \mathcal{G}_{ij}(u; u') \left(\frac{\Delta u}{2P_v} \mathcal{G}^{jl}(u; u') P_l \right) \\ &= -\frac{(\Delta u \mp i\epsilon)^2}{4P_v^2} = -(\Delta\tau \mp i\epsilon)^2 = -\frac{(\Delta t \mp i\epsilon)^2}{E^2}, \end{aligned} \quad (3.23)$$

where, for gravitational waves oscillating in the $(i, j = x, y)$ -plane, we have,

$$\mathcal{G}_{ij}(u; u') \equiv \begin{cases} \mathcal{G}_{ij}^\perp(u; u'), & \text{when } i, j = 1, 2; \\ \delta_{ij}, & \text{when } i, j = 3, \dots, D-2. \end{cases} \quad (3.24)$$

Eq. (3.23) implies that, transforming from lightcone coordinates to Cartesian coordinates is simple, and it amounts to, $(\Delta u \mp i\epsilon)/(2P_v) \rightarrow (\Delta t \mp i\epsilon)/E$, where E is the energy per unit mass. Equation (3.23) is a remarkable result, and it states that the only effect planar gravitational waves induce on inertial particles (moving along free geodesics) as seen by an Unruh-de Witt detector is through the prefactor in the Wightman function (3.28) and (3.29). Now upon inserting Eq. (2.4) into (3.18),

$$\mathcal{R}(U, \Delta E) = \frac{\hbar m^{D-2}}{(2\pi)^{\frac{D}{2}}} \int_{-\infty}^{\infty} \frac{d\Delta\tau}{[\gamma(u)\gamma(u')]^{\frac{1}{4}} \sqrt{\Upsilon(U; \Delta u)}} e^{-i\Delta E \Delta\tau} \frac{K_{\frac{D-2}{2}}(im(\Delta\tau - i\epsilon))}{(im(\Delta\tau - i\epsilon))^{\frac{D-2}{2}}}, \quad (3.25)$$

where $u = U + \Delta u/2$, $u' = U - \Delta u/2$, and we made use of Eq. (3.23), and we made use of, $m\sqrt{-(\Delta\tau - i\epsilon)^2} = im(\Delta\tau - i\epsilon)$. With Eq. (3.18) in mind, Eq. (3.25) can be also written as,

$$\mathcal{R}(U, \Delta E) = \frac{\hbar m^{D-2}}{(2\pi)^{\frac{D}{2}}} \int_0^\infty \frac{d\Delta\tau}{[\gamma(u)\gamma(u')]^{\frac{1}{4}} \sqrt{\Upsilon(U; \Delta u)}} \left[e^{-i\Delta E \Delta\tau} \frac{K_{\frac{D-2}{2}}(im(\Delta\tau - i\epsilon))}{(im(\Delta\tau - i\epsilon))^{\frac{D-2}{2}}} + \text{c.c.} \right]. \quad (3.26)$$

The principal objective of this section is to compute the transition rate in Eq. (3.25) or, equivalently, in Eq. (3.26).

Before we embark on the full calculation, let us firstly consider the simpler, massless scalar, case, whose Wightman function is obtained by taking the limit $m \rightarrow 0$ in Eq. (2.4). The following series representation of the Bessel function is handy,

$$\frac{K_\nu(z)}{z^\nu} = \frac{\Gamma(\nu)\Gamma(1-\nu)}{2^{1+\nu}} \left[\sum_{n=0}^{\infty} \frac{(z/2)^{2n-2\nu}}{n!\Gamma(n+1-\nu)} - \sum_{n=0}^{\infty} \frac{(z/2)^{2n}}{n!\Gamma(n+1+\nu)} \right], \quad (3.27)$$

where $z = m\sqrt{\Delta\bar{x}_{(\pm)}^2}$ and $\nu = (D-2)/2$. In the massless limit only the first term of the first series in Eq. (3.27) contributes, resulting in,

$$i\Delta_0^{(+)}(x; x') = \frac{\hbar\Gamma(\frac{D-2}{2})}{4\pi^{D/2}[\gamma(u)\gamma(u')]^{1/4}\sqrt{\Upsilon(u, u')}} \left(\frac{1}{\Delta\bar{x}_{(+)}^2(x; x')} \right)^{\frac{D-2}{2}}, \quad (3.28)$$

which in $D = 4$ simplifies to,

$$i\Delta_0^{(+)}(x; x') \xrightarrow{D \rightarrow 4} \frac{\hbar}{4\pi^2[\gamma(u)\gamma(u')]^{1/4}\sqrt{\Upsilon(u, u')}} \times \frac{1}{\Delta\bar{x}_{(+)}^2(x; x')}, \quad (3.29)$$

where $\Delta\bar{x}_{(+)}^2(x; x') = -(\Delta\tau - i\epsilon)^2$ is given in Eqs. (3.23).

In what follows we evaluate the integral in Eq. (3.25) for two simple cases of monochromatic planar gravitational waves. We shall firstly consider the detector transition rate for monochromatic, nonpolarized gravitational waves, and then for polarized gravitational waves.

Monochromatic nonpolarized gravitational waves. The deformation matrix (3.24) for gravitational waves in linear representation (1.2) in the (xy) -plane in the $\{U, \Delta u\}$ -coordinates, $\mathcal{G}_{ij}^\perp(U; \Delta u)$, can be inferred from Eqs. (2.10–2.11),

$$\begin{aligned} \mathcal{G}_{ij}^\perp(U; \Delta u) &= \frac{1}{\gamma\Upsilon(\Delta u)} \begin{pmatrix} 1+h\cos(\omega_g U)j_0\left(\frac{\omega_g \Delta u}{2}\right) & h\sin(\omega_g U)j_0\left(\frac{\omega_g \Delta u}{2}\right) \\ h\sin(\omega_g U)j_0\left(\frac{\omega_g \Delta u}{2}\right) & 1-h\cos(\omega_g U)j_0\left(\frac{\omega_g \Delta u}{2}\right) \end{pmatrix} \\ &= \frac{1}{\gamma\Upsilon(\Delta u)} \left[\delta_{ij}^\perp + h_{ij}^\perp(U)j_0\left(\frac{\omega_g \Delta u}{2}\right) \right], \quad (i, j = 1, 2), \end{aligned} \quad (3.30)$$

$$\gamma\Upsilon(\Delta u) \equiv \gamma \det[\Upsilon] = \frac{1}{\gamma} \left[1 - h^2 j_0^2\left(\frac{\omega_g \Delta u}{2}\right) \right], \quad (\gamma = 1 - h^2), \quad (3.31)$$

where $U = (u + u')/2$, $\Delta u = u - u'$, and $j_0(z) = \sin(z)/z$.² For nonpolarized gravitational waves the transition rate in Eq. (3.25) simplifies to,

$$\mathcal{R}(\Delta E) = \frac{\hbar m^{D-2} \sqrt{\gamma}}{(2\pi)^{\frac{D}{2}}} \int_{-\infty}^{\infty} \frac{d\Delta\tau}{\left[1 - h^2 j_0^2(P_v \omega_g \Delta\tau)\right]^{1/2}} e^{-i\Delta E \Delta\tau} \frac{K_{\frac{D-2}{2}}(im(\Delta\tau - i\epsilon))}{(im(\Delta\tau - i\epsilon))^{\frac{D-2}{2}}}, \quad (3.32)$$

where we made use of, $\Delta u = 2P_v \Delta\tau$. Notice that, for nonpolarized gravitational waves, $\mathcal{R}(\Delta E)$ does not depend on the average time U . When understood as a function of complex Δu , the integrand in Eq. (3.32) has two square-root cuts along the imaginary axis of complex $\Delta\tau$, starting at the roots of the equation,

$$j_0(P_v \omega_g \Delta\tau) = \frac{\sinh(\theta)}{\theta} = \frac{1}{h} \gg 1, \quad (3.33)$$

where $\theta = -iP_v \omega_g \Delta\tau$. For $h \ll 1$ the root $\theta_0(h)$ can be approximated by the solution of $\theta_0/(e^{\theta_0} - e^{-\theta_0}) = h/2 \ll 1 \Rightarrow (-|\theta_0|)e^{-|\theta_0|} \approx -h/2$, which can be expressed in terms of the Lambert W function (defined by the solution of, $we^w = z$),³

$$|\theta_0(h)| \approx -\Re\left[W\left(-\frac{h}{2}\right)\right], \quad (3.34)$$

such that there are two symmetric solutions.⁴ These two roots define the beginning of the square root cuts, the lower one is shown in figure 1. One can make use of the Cauchy integral formula to replace the integral in Eq. (3.32) by an equivalent integral,

$$\mathcal{R}(\Delta E) = \frac{\hbar m^{D-2} \sqrt{\gamma}}{(2\pi)^{\frac{D}{2}}} \frac{2}{P_v \omega_g} \int_{\theta_0}^{\infty} \frac{d\theta}{\left[h^2 \frac{\sinh^2(\theta)}{\theta^2} - 1\right]^{1/2}} e^{-\frac{\Delta E}{P_v \omega_g} \theta} \frac{K_{\frac{D-2}{2}}\left(\frac{m}{P_v \omega_g} \theta\right)}{\left(\frac{m}{P_v \omega_g} \theta\right)^{\frac{D-2}{2}}}, \quad (3.35)$$

²In exponential representation used in Ref. [1], in which the spatial part of the metric tensor is, $g_{ij}(u) = [\exp(\tilde{\mathbf{h}}(u))]_{ij}$, we have, $\gamma \equiv \det[g_{ij}(u)] = 1$ and $\gamma\Upsilon(u; u') = \cosh^2(\tilde{h}) - \sinh^2(\tilde{h})j_0^2(\omega_g \Delta u/2)$, such that $\gamma\Upsilon(u; u) = 1$.

³The solutions for the poles, $|\theta_0| \approx -\Re[W(-h/2)]$ can be approximated by iterating, $|\theta_0| = \ln\left(\frac{2}{h}\right) + \ln(|\theta_0|)$, giving $|\theta_0| = \ln\left(\frac{2}{h}\right) + \ln\left[\ln\left(\frac{2}{h}\right) + \ln\left(\ln\left(\frac{2}{h}\right) \dots\right)\right]$. The exact solution can be obtained by iterating, $|\theta_0| = \ln\left(\frac{2}{h}\right) + \ln\left(\frac{|\theta_0|}{2} + \sqrt{h^2 + \theta_0^2}\right)$. When $h \ll 1$, the error in the approximation by the Lambert function decreases as, $\mathcal{O}(h^2/\ln^2(h))$, such that, in the limit when $h \rightarrow 0$, the approximation by the (real part of the) Lambert function becomes exact.

⁴In exponential representation the approximate roots are given by changing Eq. (3.34) to $|\theta_0(h)| \approx -\Re[W(-\tanh(\tilde{h})/2)]$. This means that the results in exponential representation are obtained from those in linear representation by the replacement, $h \rightarrow \tanh(\tilde{h})$.

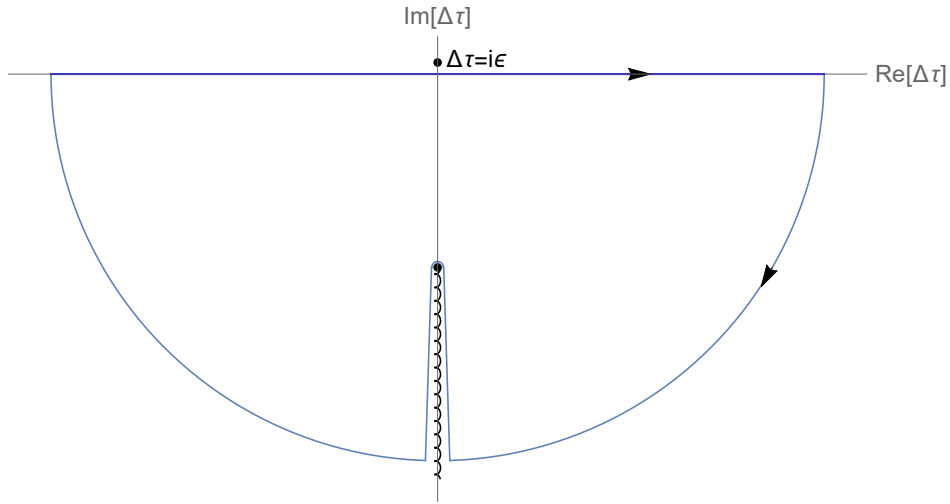


Figure 1: The complex contour used to obtain the detector transition rate in Eq. (3.16), which shows that the integral over the real axis can be replaced by the two sections along the cut in the lower complex Δu -plane.

where $\theta_0 > 0$ is the positive root of Eq. (3.34), we made use of the fact that the integral over the entire contour in figure 1 vanishes and, in the last step, made the replacement, $\theta \rightarrow -\theta$. This integral is finite, so one can set $D = 4$,

$$\mathcal{R}(\Delta E) = \frac{\hbar m \sqrt{\gamma}}{2\pi^2} \int_{\theta_0}^{\infty} \frac{d\theta}{[h^2 \sinh^2(\theta) - \theta^2]^{1/2}} e^{-\frac{\Delta E}{P_v \omega_g} \theta} K_1\left(\frac{m}{P_v \omega_g} \theta\right), \quad (3.36)$$

which in the massless limit this reduces to,

$$\mathcal{R}(\Delta E) = \frac{\hbar \sqrt{\gamma} P_v \omega_g}{2\pi^2} \int_{\theta_0}^{\infty} \frac{d\theta}{\theta [h^2 \sinh^2(\theta) - \theta^2]^{1/2}} e^{-\frac{\Delta E}{P_v \omega_g} \theta}. \quad (3.37)$$

The integrals in Eqs. (3.36–3.37) are hard, and cannot be evaluated analytically. Let us firstly consider the easier, massless case.

Two analytic approximations can be used for the transition rate in Eq. (3.32), an expansion in powers of h^2 and an expansion around the beginning of the cut, the latter increasing in accuracy in the large energy limit, when $\Delta E \gg P_v \omega_g$. The first approximation amounts to setting $D = 4$ and expanding (3.32) in powers of h^2 . This replaces the cut contribution by a sum over the poles at $\Delta u = i\epsilon$ of the order $2n + 2$,

$$\mathcal{R}(\Delta E) = \frac{\hbar m^2 \sqrt{\gamma}}{4\pi^2} \frac{1}{\sqrt{\pi}} \sum_{n=1}^{\infty} \Gamma\left(n + \frac{1}{2}\right) \frac{h^{2n}}{n!} \int_{-\infty}^{\infty} \frac{d\Delta\tau}{(P_v \omega_g \Delta\tau)^{2n}} \sin^{2n}(P_v \omega_g \Delta\tau) e^{-i\Delta E \Delta\tau} \frac{K_1(im(\Delta\tau - i\epsilon))}{im(\Delta\tau - i\epsilon)}, \quad (3.38)$$

which can be evaluated by making use of the Cauchy integral formula. The integration of the n th term in the sum does not vanish provided $\Delta E - 2nP_v \omega_g < 0$. In the massless limit the last term in Eq. (3.32) simplifies to, $-1/[m(\Delta\tau - i\epsilon)]^2$, such that the integral evaluates to,

$$\begin{aligned} \mathcal{R}(\Delta E) = & \frac{\hbar \sqrt{\gamma} P_v \omega_g}{2\pi^2} \left\{ \frac{\pi}{6} h^2 \left(1 - \frac{\Delta E}{2P_v \omega_g}\right)^3 \Theta(2P_v \omega_g - \Delta E) \right. \\ & \left. + \frac{\pi}{5} h^4 \left[-\frac{1}{8} \left(1 - \frac{\Delta E}{2P_v \omega_g}\right)^3 \Theta(2P_v \omega_g - \Delta E) + \left(1 - \frac{\Delta E}{4P_v \omega_g}\right)^3 \Theta(4P_v \omega_g - \Delta E) \right] + \mathcal{O}(h^6) \right\}, \end{aligned} \quad (3.39)$$

where we made use of, $\sin^2(z) = \frac{1}{2} - \frac{1}{4}(e^{2iz} + e^{-2iz})$, and we have assumed that, $\Delta E > 0$ and $P_v > 0$.

The second analytic approximation can be obtained by expanding the integrand in Eq. (3.37) around the beginning of the cut. The result is,

$$\mathcal{R}(\Delta E) \approx \frac{\hbar\sqrt{\gamma}P_v\omega_g}{2\pi^2} \sqrt{\frac{P_v\omega_g}{\Delta E}} \left(\frac{\hbar}{2}\right)^{\frac{\Delta E}{P_v\omega_g}} \frac{1}{\left[\ln\left(\frac{2}{\hbar}\right) + \ln\left(\ln\left(\frac{2}{\hbar}\right)\right)\right]^{2+\frac{\Delta E}{P_v\omega_g}}} \left[1 + \mathcal{O}\left(\frac{P_v\omega_g}{\Delta E}\right)\right]. \quad (3.40)$$

One can evaluate Eq. (3.37) numerically, and the results are shown in figure 2. In figure 3 we compare

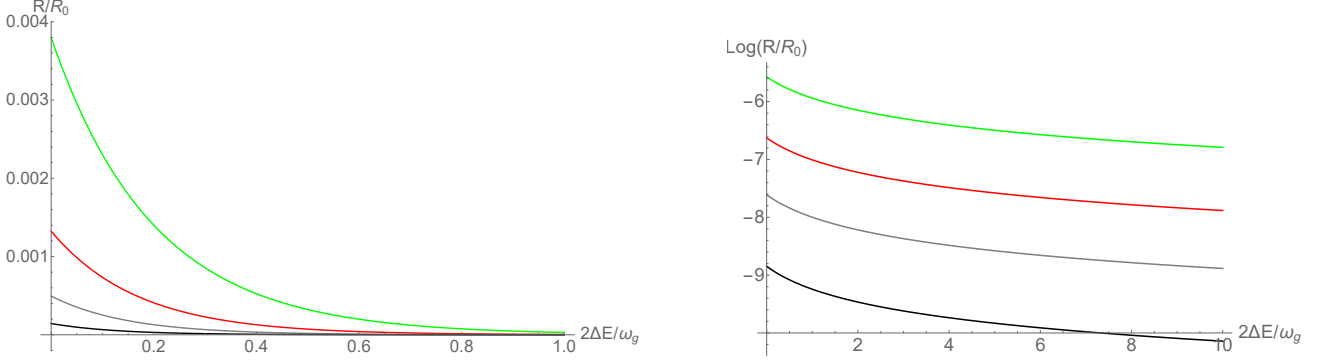


Figure 2: *Left panel:* The transition rate \mathcal{R} in Eq. (3.37) for a massless scalar as a function of $\Delta E/(P_v\omega_g)$ in units of $\mathcal{R}_0 = \hbar\sqrt{1-h^2}P_v\omega_g/(2\pi^2)$ as measured by the Unruh-de Witt detector. Different curves are for different values of the gravitational strain (from top down): $h = 0.1$ (green), $h = 0.05$ (red), $h = 0.025$ (gray), and $h = 0.01$ (black). *Right panel:* The same diagram for $\ln(\mathcal{R}/\mathcal{R}_0) + \Delta E\theta_0/(P_v\omega_g)$, where $\theta_0 > 0$ is the imaginary pole at the beginning of the square root cut in Eq. (3.33).

the numerical results for the transition rate with two analytical approximations. The first approximation is obtained by expanding in powers of h^2 (dashed lines in figure 3) and the second by expanding around the beginning of the cut (dotted lines in figure 3). Both approximations are reasonable, but neither is accurate. The second approximation captures correctly the large ΔE behaviour, $\mathcal{R}(\Delta E) \propto \exp\left[-\frac{\Delta E}{P_v\omega_g}\theta_0\right]$, meaning that the transition rate is exponentially suppressed with growing $\left[\frac{\Delta E}{P_v\omega_g}\theta_0\right]$, but the analytical estimate poorly approximates the constant in front of the exponential. Due to the complicated dependence of $\theta_0(h)$ on h in Eq. (3.34), the dependence of the transition rate on h is nonanalytic, which explains why expanding in powers of h^2 performs relatively poorly. This kind of nonanalytic behavior is hard to guess, and impossible to obtain without knowing the scalar Wightman function from Ref. [1], which resums the gravitational wave insertions.

Switching on the scalar mass suppresses the transition rate further, and the results obtained by numerically integrating (3.36) for $m = P_v\omega_g$ shown in figure 4 are significantly suppressed when compared with those for the massless scalar in figures 2 and 3. Just as in the massless case, at large ΔE , the results decay exponentially as, $\mathcal{R} \propto \exp\left[\frac{\Delta E}{P_v\omega_g}\theta_0\right]$, and in the limit of a large mass, $m\theta_0 \gg P_v\omega_g$, there is an additional exponential suppression, $\mathcal{R} \propto \exp\left[\frac{(\Delta E+m)}{P_v\omega_g}\theta_0\right]$. To see that, let us approximately evaluate the integral in Eq. (3.36) by expanding around the beginning of the cut at $\theta = \theta_0(h)$,

$$\begin{aligned} \mathcal{R}(\Delta E) &= \frac{\hbar\sqrt{\gamma}m}{2\pi^2} \sqrt{\frac{\pi P_v\omega_g}{2\Delta E\theta_0(\theta_0-1)}} K_1\left(\frac{m\theta_0}{P_v\omega_g}\right) e^{-\frac{\Delta E\theta_0}{P_v\omega_g}} \\ &\times \left\{1 - \frac{P_v\omega_g}{2\Delta E} \left[\frac{2\theta_0^2-1}{4\theta_0(\theta_0-1)} + \frac{m}{P_v\omega_g} \frac{K_2\left(\frac{m\theta_0}{P_v\omega_g}\right)}{K_1\left(\frac{m\theta_0}{P_v\omega_g}\right)} - \frac{1}{\theta_0}\right] + \mathcal{O}(\Delta E^{-2})\right\}, \end{aligned} \quad (3.41)$$

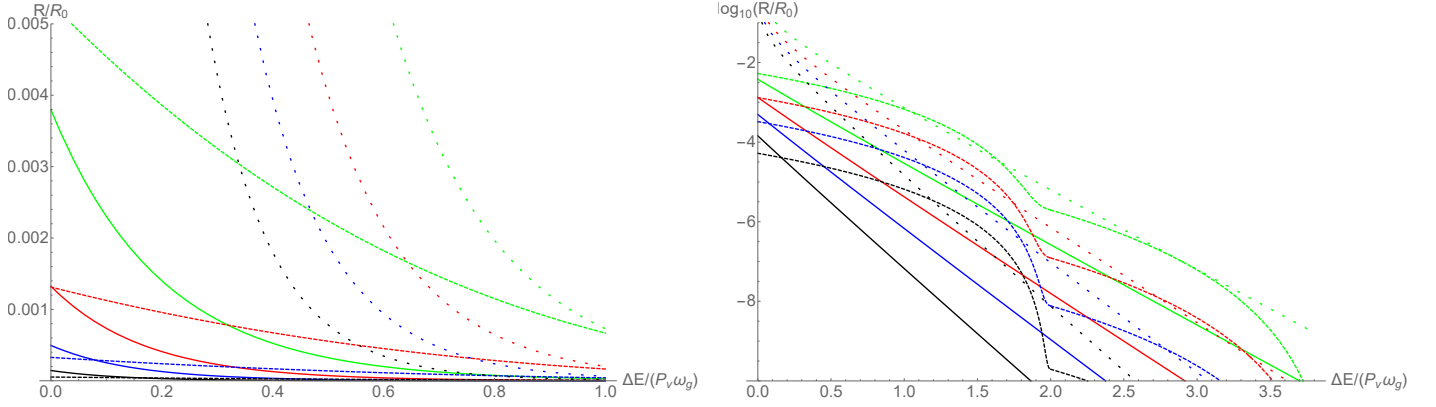


Figure 3: *Left panel:* The detector transition rate \mathcal{R} for a massless scalar as function of $\Delta E/(P_v \omega_g)$ in units of $\mathcal{R}_0 = \hbar \sqrt{1 - h^2} P_v \omega_g / (2\pi^2)$ as measured by the Unruh-de Witt detector. Different curves are for different values of the gravitational strain: $h = 0.1$ (green), $h = 0.05$ (red), $h = 0.025$ (blue), and $h = 0.01$ (black). Solid lines show numerical results, dashed lines are approximate curves in Eq. (3.39), obtained by expanding the integrand in powers of h^2 , and dotted lines represent the function in Eq. (3.40), obtained by expanding the integrand around the beginning of the cut. *Right panel:* The same diagram for $\log_{10}(\mathcal{R}/\mathcal{R}_0)$.

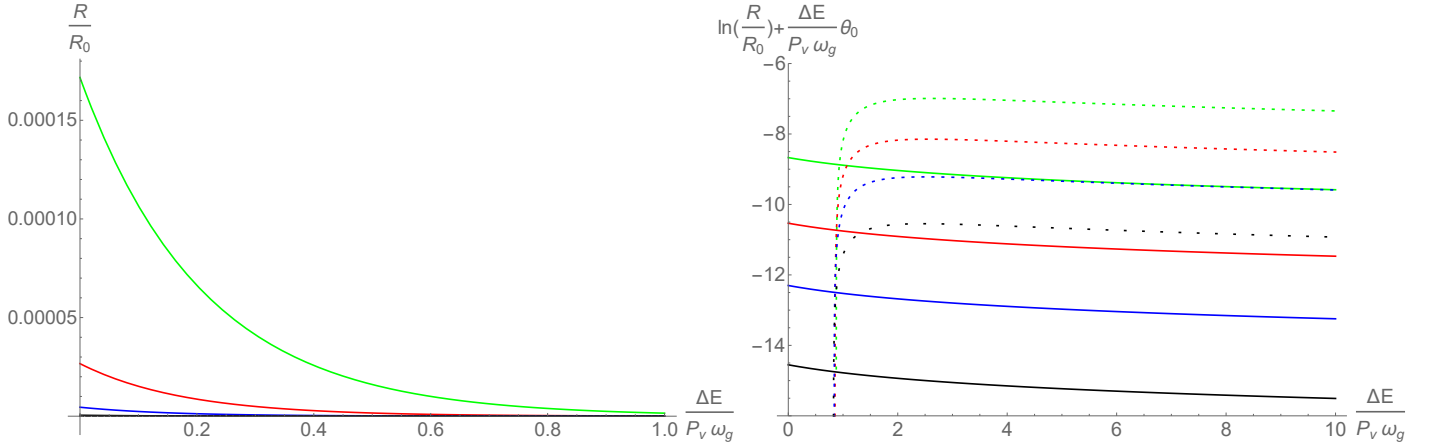


Figure 4: *Left panel:* The detector transition rate $\mathcal{R}(\Delta E)$ for a massive scalar with $m = P_v \omega_g$ as function of $\Delta E/(P_v \omega_g)$ in units of $\mathcal{R}_0 = \hbar \sqrt{1 - h^2} P_v \omega_g / (2\pi^2)$ as measured by the Unruh-de Witt detector. Different curves are for different values of the gravitational strain: $h = 0.1$ (green), $h = 0.05$ (red), $h = 0.025$ (blue), and $h = 0.01$ (black). *Right panel:* The same diagram for $\ln(\mathcal{R}/\mathcal{R}_0) + (\Delta E \theta_0)/(P_v \omega_g)$.

which applies when $\Delta E \theta_0 / (P_v \omega_g) \gg 1$, and where we dropped the term $h^2 / (2\theta_0)$ in the expansion, $\sqrt{\theta_0^2 + h^2} \simeq \theta_0 + \mathcal{O}(h^2 / \theta_0)$. This amounts to approximating the position of the cut, $\theta = \theta_0(h)$, by the Lambert function in Eq. (3.34). We shall not attempt to evaluate the integrals in Eq. (3.38) for the massive case, as that would require not only to account for the contributions of the poles at $\Delta u = i\epsilon$, but also for the contribution of the logarithmic cut of the modified Bessel function, $im(\Delta u - i\epsilon) K_1(im(\Delta u - i\epsilon))$, which extends from $\Delta u = 0$ to $0 + i\infty$. Finally, in figure 5 we show the same transition rate as in figure 4, but now as a function of the mass for a fixed $\Delta E = 2P_v \omega_g$ (left panel) and $\Delta E = 10P_v \omega_g$ (right panel). The figure shows that the transition rate is exponentially suppressed by the mass as, $\mathcal{R} \sim e^{-m\theta_0(h)/(P_v \omega_g)}$, which can be also inferred from the asymptotic expansion of the Bessel function in Eq. (3.41), $K_1\left(\frac{m\theta_0}{P_v \omega_g}\right) \sim \sqrt{\frac{\pi P_v \omega_g}{2m\theta_0}} \exp\left(-\frac{m\theta_0}{P_v \omega_g}\right)$.

Monochromatic polarized gravitational waves. Here we shall consider polarized gravitational

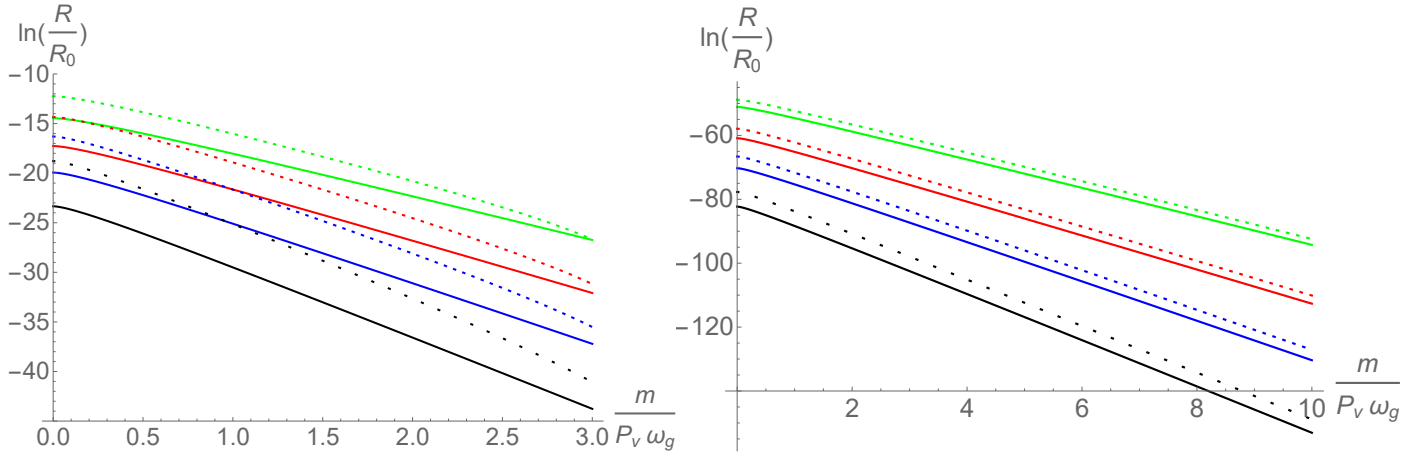


Figure 5: *Left panel:* The detector transition rate \mathcal{R} for a massive scalar with $\Delta E/(P_v \omega_g) = 2$ as a function of $m/(P_v \omega_g)$ in units of $\mathcal{R}_0 = \hbar \sqrt{1 - h^2} P_v \omega_g / (2\pi^2)$ as measured by the Unruh-de Witt detector. Different curves are for different values of the gravitational strain: $h = 0.1$ (green), $h = 0.05$ (red), $h = 0.025$ (blue), and $h = 0.01$ (black). *Right panel:* The same but with $\Delta E/(P_v \omega_g) = 10$. The solid curves are numerical results, and the short dashed curves are the approximation in Eq. (3.41).

waves, whose analysis is much trickier, as the interaction with the detector depends on the average time variable, $U = (u + u')/2$. Let us begin our analysis by noting that Eq. (2.8) can be recast as,

$$\Upsilon_{ij}(U, \Delta u) = \sum_{n=0}^{\infty} \left[\frac{\partial^{2n}}{\partial U^{2n}} g^{ij}(U) \right] \frac{(\Delta u/2)^{2n}}{(2n+1)!}, \quad (3.42)$$

where $\Delta u = u - u'$, and $g^{ij}(U)$ denotes the inverse of $g_{ij}(U)$, which for generally polarized waves (fluctuating in a 2 dimensional plane) takes the form (*cf.* Eq. (2.9)),

$$g^{ij}(U) = \frac{1}{1 - h_+^2 c_+^2 - h_\times^2 c_\times^2} \begin{pmatrix} 1 - h_+ c_+ & -h_\times c_\times \\ -h_\times c_\times & 1 + h_+ c_+ \end{pmatrix}, \quad (3.43)$$

where $c_+(U) = \cos(\omega_g U + \psi/2)$, $c_\times(U) = \cos(\omega_g U - \psi/2)$, where ψ is an arbitrary phase (in the case of nonpolarized gravitational waves, $\psi = \pi/2$). Evaluating (3.42) for g^{ij} in Eq. (3.43) is a formidable task, and we shall content ourselves by evaluating $\Upsilon_{ij}(u; u')$ to the quadratic order in h_+ and h_\times ,

$$\begin{aligned} \Upsilon_{ij}(U; \Delta u) &= \begin{pmatrix} 1 & 0 \\ 0 & 1 \end{pmatrix} \left[1 + \frac{h_+^2}{2} \left(1 + (2c_+^2 - 1)j_0(\omega_g \Delta u) \right) + \frac{h_\times^2}{2} \left(1 + (2c_\times^2 - 1)j_0(\omega_g \Delta u) \right) \right] \\ &+ \begin{pmatrix} -h_+ c_+ & -h_\times c_\times \\ -h_\times c_\times & h_+ c_+ \end{pmatrix} j_0 \left(\frac{\omega_g \Delta u}{2} \right) + \mathcal{O}(h_+^2 h_\times, h_+ h_\times^2), \end{aligned} \quad (3.44)$$

whose determinant equals,

$$\begin{aligned} \Upsilon(U; \Delta u) &= 1 - h_+^2 \left[c_+^2 j_0^2 \left(\frac{\omega_g \Delta u}{2} \right) - 1 - (2c_+^2 - 1)j_0(\omega_g \Delta u) \right] \\ &- h_\times^2 \left[c_\times^2 j_0^2 \left(\frac{\omega_g \Delta u}{2} \right) - 1 - (2c_\times^2 - 1)j_0(\omega_g \Delta u) \right] + \mathcal{O}(h_+^2 h_\times, h_+ h_\times^2). \end{aligned} \quad (3.45)$$

In the nonpolarized case, in which $\psi = \pi/2$ and $h_+ = h_\times = h$, this reduces to, $\Upsilon(U; \Delta u) \rightarrow 1 - h^2 \left[j_0^2 \left(\frac{\omega_g \Delta u}{2} \right) + 2 \right]$, which agrees with Eq. (3.31) when one recalls that, $1/\gamma^2 = 1 + 2h^2 + \mathcal{O}(h^4)$. Upon

introducing $\tilde{\gamma}(h_+, h_\times) = 1 - \frac{h_+^2 + h_\times^2}{2}$, Eq. (3.45) can be recast as,

$$\Upsilon(U; \Delta u) = \frac{1}{\tilde{\gamma}^2} \left\{ 1 - \left[(h_+^2 c_+^2 + h_\times^2 c_\times^2) j_0^2 \left(\frac{\omega_g \Delta u}{2} \right) - (h_+^2 (2c_+^2 - 1) + h_\times^2 (2c_\times^2 - 1)) j_0(\omega_g \Delta u) \right] \right\} + \mathcal{O}(h_+^2 h_\times, h_+ h_\times^2). \quad (3.46)$$

To complete the analysis, we also need,

$$\sqrt{\gamma(u)\gamma(u')} = \tilde{\gamma} - \frac{1}{2} (h_+^2 (2c_+^2 - 1) + h_\times^2 (2c_\times^2 - 1)) \cos(\omega_g \Delta u) + \mathcal{O}(h_+^2 h_\times, h_+ h_\times^2), \quad (3.47)$$

which, when multiplied with (3.46), gives,

$$\begin{aligned} \sqrt{\gamma(u)\gamma(u')} \Upsilon(U; \Delta u) &= \frac{1}{\tilde{\gamma}} \left\{ 1 - \left[(h_+^2 c_+^2 + h_\times^2 c_\times^2) j_0^2 \left(\frac{\omega_g \Delta u}{2} \right) \right. \right. \\ &\quad \left. \left. - (h_+^2 (2c_+^2 - 1) + h_\times^2 (2c_\times^2 - 1)) \left(j_0(\omega_g \Delta u) - \frac{1}{2} \cos(\omega_g \Delta u) \right) \right] \right\} + \mathcal{O}(h_+^2 h_\times, h_+ h_\times^2). \end{aligned} \quad (3.48)$$

This product appears in the propagator in Eq. (3.25), and generates square-root cuts ⁵, just as in the nonpolarized waves in Eq. (3.32). The integral can be evaluated by contour integration, with the contour showed in figure 1, resulting in the cut contribution (*cf.* Eq. (3.36)),

$$\mathcal{R}(U, \Delta E) = \frac{\hbar m \sqrt{\tilde{\gamma}}}{2\pi^2} \int_{\theta_0}^{\infty} \frac{d\theta}{[H^2(U, \theta) - \theta^2]^{1/2}} e^{-\frac{\Delta E}{P_v \omega_g} \theta} K_1\left(\frac{m}{P_v \omega_g} \theta\right), \quad (3.49)$$

where $h^2(U) = h_+^2 c_+^2(U) + h_\times^2 c_\times^2(U)$,

$$H^2(U, \theta) = h^2(U) \sinh^2(\theta) + \left[h^2(U) - \frac{h_+^2 + h_\times^2}{2} \right] \left[\theta^2 \cosh(2\theta) - \theta \sinh(2\theta) \right], \quad (3.50)$$

and $\theta_0 > 0$ denotes the beginning of the cut defined by, $H^2(U, \theta_0) = \theta_0^2$. Next we insert,

$$h^2(U) = \frac{h_+^2 + h_\times^2}{2} + \frac{h_+^2 - h_\times^2}{2} \cos(2\omega_g U) c_\psi - \frac{h_+^2 - h_\times^2}{2} \sin(2\omega_g U) s_\psi, \quad (c_\psi = \cos(\psi), s_\psi = \sin(\psi)), \quad (3.51)$$

into Eq. (3.50) to obtain,

$$\begin{aligned} \left[\frac{h_+^2 + h_\times^2}{2} c_\psi \cos(2\omega_g U) - \frac{h_+^2 - h_\times^2}{2} s_\psi \sin(2\omega_g U) \right] \left[\sinh^2(\theta_0) + \theta_0^2 \cosh(2\theta_0) - \theta_0 \sinh(2\theta_0) \right] \\ + \frac{h_+^2 + h_\times^2}{2} \sinh^2(\theta_0) - \theta_0^2 = 0. \end{aligned} \quad (3.52)$$

Because of the U dependence, Eq. (3.52) may or may not have a solution, meaning that the cuts exist only when (3.52) can be solved for some real U . To simplify our analysis, recall that we are interested in the limit when, $h_+, h_\times \ll 1$, in which case in most of the parameter space $\theta_0 \gg 1$, and one can

⁵Our analysis is accurate at the order h^2 , and thus not exact. Therefore, one should be aware of the possibility that polarized gravitational wave may generate a more baroque cuts in the complex Δu plane, for an illustration see Appendix B.

approximate Eq. (3.52) by keeping the leading order terms $\propto e^{2\theta_0}$ only.⁶ Multiplying Eq. (3.52) by $2e^{-2\theta_0}/\cos^2(\omega_g U) = 2e^{-2\theta_0}(1+t^2)$ and neglecting the terms suppressed as $\sim e^{-2n\theta_0}$ ($n = 1, 2$) yields a quadratic equation for $t = \tan(\omega_g U)$,

$$at^2 - 2bt + c > 0 \implies a(t - t_+)(t - t_-) > 0, \quad t_{\pm} = \frac{1}{a}[b \pm \sqrt{\Delta}], \quad \Delta = b^2 - ac, \quad (3.53)$$

where

$$a = \frac{h_+^2 + h_{\times}^2}{2} \left[-\left(\theta_0^2 - \theta_0 + \frac{1}{2}\right) c_{\psi} + \frac{1}{2} \right], \quad b = \frac{h_+^2 - h_{\times}^2}{2} \left(\theta_0^2 - \theta_0 + \frac{1}{2}\right) s_{\psi}, \quad c = \frac{h_+^2 + h_{\times}^2}{2} \left[\left(\theta_0^2 - \theta_0 + \frac{1}{2}\right) c_{\psi} - \frac{1}{2} \right], \quad (3.54)$$

and we made use of, $\cos(2\omega_g U) = (1 - t^2)/(1 + t^2)$ and $\sin(2\omega_g U) = 2t/(1 + t^2)$. The discriminant in Eq. (3.53) is then,

$$\begin{aligned} \Delta &= \left(\frac{h_+^2 + h_{\times}^2}{2}\right)^2 \left[\left(\theta_0^2 - \theta_0 + \frac{1}{2}\right)^2 - \frac{1}{4} \right] - h_+^2 h_{\times}^2 \left(\theta_0^2 - \theta_0 + \frac{1}{2}\right)^2 s_{\psi}^2 \\ &= \left(\frac{h_+^2 - h_{\times}^2}{2}\right)^2 \left[\left(\theta_0^2 - \theta_0 + \frac{1}{2}\right)^2 - \frac{1}{4} \right] + h_+^2 h_{\times}^2 \left[\left(\theta_0^2 - \theta_0 + \frac{1}{2}\right)^2 c_{\psi}^2 - \frac{1}{4} \right]. \end{aligned} \quad (3.55)$$

The roots t_{\pm} in Eq. (3.53) of the equation, $at^2 - 2bt + c = 0$, are real if $\Delta \geq 0$, from which we conclude that the inequality in Eq. (3.53) is satisfied:

- (1) when $a > 0$ and $\Delta < 0$: the inequality in Eq. (3.53) is satisfied for all $U \in \mathbb{R}$;
- (2) when $a > 0$ and $\Delta \geq 0$: the inequality in Eq. (3.53) is satisfied for $t = \tan(\omega_g U) < t_-$ and $\tan(\omega_g U) > t_+$;
- (3) when $a < 0$ and $\Delta \geq 0$: the inequality in Eq. (3.53) is satisfied for $t_- < \tan(\omega_g U) < t_+$;
- (4) when $a < 0$ and $\Delta < 0$: the inequality in Eq. (3.53) is never satisfied.

From Eqs. (3.54) and (3.55) we then see that $a \leq 0$ and $\Delta \geq 0$ imply,

$$\cos(\psi) \leq \frac{1}{2\theta_0(\theta_0 - 1) + 1} \simeq \frac{1}{2\theta_0^2} \quad (3.56)$$

$$\cos^2(\psi) \geq \frac{1}{[2\theta_0(\theta_0 - 1) + 1]^2} - \frac{1}{4} \left(\frac{h_+}{h_{\times}} - \frac{h_{\times}}{h_+}\right)^2 \left[1 - \frac{1}{[2\theta_0(\theta_0 - 1) + 1]^2} \right] \simeq \frac{1}{4\theta_0^4} - \frac{1}{4} \left(\frac{h_+}{h_{\times}} - \frac{h_{\times}}{h_+}\right)^2,$$

where the last inequalities represent good approximations when $\theta_0 \gg 1$. Notice that if,

$$\left| \frac{h_+}{h_{\times}} - \frac{h_{\times}}{h_+} \right| > \frac{1}{\sqrt{\theta_0(\theta_0 - 1)(\theta_0^2 - \theta_0 + 1)}} \simeq \frac{1}{\theta_0(\theta_0 - 1)} \implies \Delta > 0, \quad (3.57)$$

and options (1) and (4) are absent, and an Unruh-de Witt detector gets excited only during parts of the period. For nonpolarized gravitational waves, $\cos(\psi) = 0$, and excitations occur when,

$$t_- < \tan(\omega_g U) < t_+. \quad (3.58)$$

⁶The same approximation was shown to work extremely well when we analysed the nonpolarized case.

There is another important difference between detector's transition rate induced by nonpolarized and polarized gravitational waves. Upon rewriting Eq. (3.52) at leading order in $e^{2\theta_0}$,

$$\frac{h_+^2 + h_\times^2}{2} + \left[\frac{h_+^2 + h_\times^2}{2} c_\psi \cos(2\omega_g U) - \frac{h_+^2 - h_\times^2}{2} s_\psi \sin(2\omega_g U) \right] \left[2\theta_0(\theta_0 - 1) + 1 \right] + \mathcal{O}(e^{-2\theta_0}) = 4\theta_0^2 e^{-2\theta_0}, \quad (3.59)$$

we see that only the first term in Eq. (3.59) survives in the nonpolarized case, in which $h_+ = h_\times$ and $\cos(\psi) = 0$. Very close to that point, the first term $(h_+^2 + h_\times^2)/2$ dominates, and the beginning of the cut is still well approximated in terms of the Lambert function as (*cf.* Eq. (3.34)),

$$\theta_0(h_+, h_\times) \simeq -\Re \left[W \left(-\frac{1}{2} \sqrt{\frac{h_+^2 + h_\times^2}{2}} \right) \right], \quad (3.60)$$

whose small $\bar{h} \equiv \sqrt{(h_+^2 + h_\times^2)}/2$ -expansion is highly nonanalytic. On the other hand, when deviations from the nonpolarized case are significant, the solution changes to,

$$\theta_0(h_+, h_\times) \simeq -\frac{1}{2} \ln \left[\frac{h_+^2 + h_\times^2}{4} c_\psi \cos(2\omega_g U) - \frac{h_+^2 - h_\times^2}{4} s_\psi \sin(2\omega_g U) \right], \quad (3.61)$$

which exists when the argument of the logarithm is positive, *i.e.* when $\tan(2\omega_g U) \leq \left(\frac{h_+^2 + h_\times^2}{h_+^2 - h_\times^2} \right) \cot(\psi)$ for $(h_+^2 - h_\times^2) \sin(\psi) \leq 0$.

With these considerations in mind, one can obtain an approximate expression for the detector rate in the massless limit (*cf.* Eq. (3.40)),

$$\mathcal{R}(U, \Delta E) \approx \frac{\hbar \sqrt{\gamma} P_v \omega_g}{2\pi^2} \sqrt{\frac{P_v \omega_g}{\Delta E}} \left(\frac{h_+^2 c_+^2(U) + h_\times^2 c_\times^2(U)}{2} - \frac{h_+^2 + h_\times^2}{4} \right)^{\frac{\Delta E}{2P_v \omega_g}} \Theta_+, \quad (3.62)$$

where $\Theta_+ = 1$ when the argument inside the brackets is positive, and $\Theta_+ = 0$ when it is negative. A second perturbative approximation can be obtained by expanding the integrand in Eq. (3.25) in powers of the gravitational strain. Making use of Eq. (3.48) and keeping, for simplicity, the quadratic order terms only, one obtains for the detector's transition rate in the massless scalar case,

$$\begin{aligned} \mathcal{R}(\Delta E) &= \frac{\hbar \sqrt{\gamma} P_v \omega_g}{2\pi} \left\{ \frac{h^2(U)}{6} \left(1 - \frac{\Delta E}{2P_v \omega_g} \right)^3 + \frac{2h^2(U) - (h_+^2 + h_\times^2)}{4} \left(1 - \frac{\Delta E}{2P_v \omega_g} \right) \frac{\Delta E}{2P_v \omega_g} \right\} \Theta(2P_v \omega_g - \Delta E) \\ &+ \mathcal{O}(h_{+, \times}^4), \end{aligned} \quad (3.63)$$

where $h^2(U) = h_+^2 c_+^2(U) + h_\times^2 c_\times^2(U)$, and we have dropped the quartic terms as they are significantly more complicated than in the nonpolarized case in Eq. (3.39).

In figure 6 we show selected numerical results of integrating Eq. (3.49) in the massless limit, in which the transition rate reduces to (*cf.* Eq. (3.37)),

$$\mathcal{R}(\Delta E) = \frac{\hbar \sqrt{\gamma} P_v \omega_g}{2\pi^2} \int_{\theta_0}^{\infty} \frac{d\theta}{\theta [H^2(U, \theta) - \theta^2]^{1/2}} e^{-\frac{\Delta E}{P_v \omega_g} \theta}. \quad (3.64)$$

In the same figure, for comparison, we also show the analytical estimates from Eq. (3.62) (dashed) and from Eq. (3.63) (dotted). Notice that the latter approximation (obtained by expanding in powers of h) does not work as well as in the nonpolarized case, as it need not give a positive result in the whole

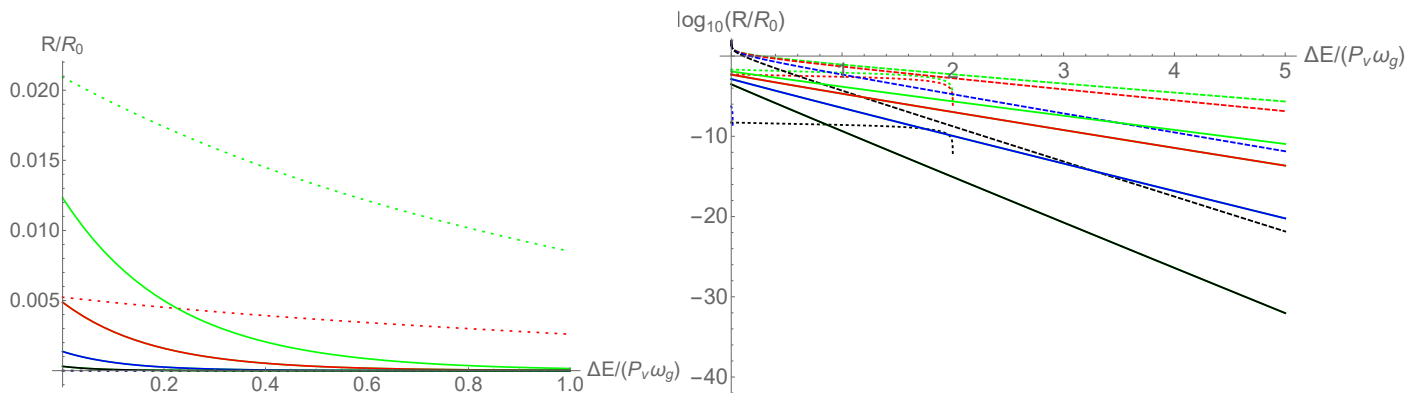


Figure 6: *Left panel:* The detector’s transition rate \mathcal{R} for a massless scalar as a function of $\Delta E/(P_v \omega_g)$ in units of $\mathcal{R}_0 = \hbar \sqrt{\gamma} P_v \omega_g / (2\pi^2)$ as measured by a freely falling Unruh-de Witt detector. All curves are for the moment in time, $U = \pi/4\omega_g$ and for the relative phase, $\psi = \pi/2$, which is the same phase difference as for nonpolarized waves. Different curves are for different values of the gravitational strains: $h_+ = 0.1$ and $h_\times = 0.2$ (green), $h_+ = 0.01$ and $h_\times = 0.1$ (red), $h_+ = 0.01$ and $h_\times = 0.001$ (blue), and $h_+ = 0$ and $h_\times = 0.0001$ (black). *Right panel:* The same but now for $\log_{10}[\mathcal{R}/\mathcal{R}_0]$. The solid curves are numerical results, the dashed curves are obtained by using the approximation in Eq. (3.62), and the dotted lines correspond to the approximation in Eq. (3.63).

interval, $0 \leq \Delta E \leq 2P_v \omega_g$.⁷ The detector’s transition rate for a massive scalar field can be studied analogously, and therefore we leave it as an exercise.

None of the results presented in this section can be compared with those in Ref. [9], where approximations were used which do not capture the effects of the cuts in figure 1.⁸

4 Conclusions and outlook

In section 2 we generalize the massive real scalar field propagator of Ref. [1] to general gravitational waves propagating in one direction, thus relaxing the monochromatic approximation used in Ref. [1]. The Wightman two-point functions are given in Eq. (2.4) and the propagator in Eqs. (2.14–2.15). We then show that the generalized propagator produces the one-loop results which are identical in form to the ones obtained in Ref. [1].

In section 3 we then study how a freely falling Unruh-de Witt detector (which couples to a massless or massive scalar field) responds to the gravitational wave background. We find that the deformation of the invariant distance induced by the gravitational waves gets fully compensated by the motion of a freely falling detector, thus leaving the effect of the modified amplitude of vacuum fluctuations expressed by the (u, u') –dependent prefactor in Eq. (2.4), the effects of which we study in some detail. We treat the detector’s transition rate in 3 different approximations:

⁷The perturbative rate can be negative if $h^2(U) < (h_+^2 + h_\times^2)/2$ and when $x_- < \Delta E/(2P_v \omega_g) < \min[x_+, 1]$, where x_\pm are the roots of the equation, $x^2 + 2[2 - 3(h_+^2 + h_\times^2)/(2h^2(U))]x + 1 = 0$.

⁸Here we do not take account of the detector’s rate induced by transitions to lower energy states considered in Ref. [9], for which $\Delta E < 0$, as those are absent when the detector is in its ground state, and moreover such transitions would be hard to resolve from detector’s response in Minkowski vacuum. The transitions we consider excite the detector, $\Delta E > 0$, and they are completely absent in Minkowski vacuum.

- *Numerical solution*, which can be considered to be exact. The resulting transition rate \mathcal{R} is exponentially suppressed, and can be approximated by, $\mathcal{R} = \mathcal{R}_0(\Delta E, m, \omega_g) \exp\left[-\frac{\Delta E}{P_v \omega_g} \theta_0(h)\right]$, where $\theta_0(h) > 0$ is the beginning of the cut in the complex Δu plane, whose functional dependence on h is determined by Eq. (3.33), and it is highly nonanalytic; $\mathcal{R}_0(\Delta E, m, \omega_g)$ is a weak function of $\Delta E/(P_v \omega_g)$ and exponentially decays with increasing $m/(P_v \omega_g)$.
- Expanding in powers of h^2 , where h is the gravitational wave strain. This generates a series of poles of the order $2n + 2$, each of which contributes to the term $\sim h^{2n}$ when $0 \leq \Delta E \leq 2nP_v \omega_g$, the first two contributions are shown in Eq. (3.39) for nonpolarized gravitational waves and in Eq. (3.63) for polarized gravitational waves.

The field theoretic interpretation of these contributions is that they actively contribute when the scalar field absorbs $2n$ gravitons, each of which with energy $P_v \omega_g$, such that the detector's energy can increase by $\Delta E \leq 2nP_v \omega_g$. Figures 3 and 6 show that expanding in powers of the gravitational wave strain captures correctly the qualitative trend of the numerical solution, but at the quantitative level this approximation performs quite poorly.

- Expanding around the cut at $\theta = \theta_0(h)$ in Eqs. (3.33) and (3.52) for nonpolarized and polarized gravitational waves, respectively. The leading order result is shown in Eq. (3.40) for nonpolarized waves and in Eq. (3.62) for polarized waves. This approximation models correctly the exponential decay with increasing ΔE of the detector's transition rate, that is its nonanalytic structure in the gravitational wave strain, but it fails to correctly model the exponential prefactor, as can be clearly seen from figures 3, 4, 5 and 6.

In this work we have addressed the response of an Unruh-de Witt detector to monochromatic, unidirectional, nonpolarized and polarized, gravitational waves. A more general investigation is warranted by relaxing any of the above mentioned restrictions. It would be, in particular, of interest to calculate the transition rate of the detector to a stochastic gravitational wave background. But to do that properly requires knowledge of the corresponding propagator, which is presently unknown.

5 Appendices

Appendix A: The method of mode sums

Here we briefly recap how to construct the Wightman functions by using the method of mode sums. Upon expanding the scalar field operator are expanded in terms of the momentum space mode functions and creation and annihilation operators, one obtains the following expressions for the positive and negative frequency Wightman functions,

$$i\Delta^{(+)}(x; x') = \langle \Omega | \hat{\phi}(x) \hat{\phi}(x') | \Omega \rangle = \int \frac{d^{D-1}k}{(2\pi)^{D-1}} e^{i\vec{k}_\perp \cdot \Delta\vec{x}_\perp - \frac{i}{2}\Omega_-(\vec{k})\Delta v} \phi_+(u, \vec{k}) \phi_-(u', -\vec{k}), \quad (5.1)$$

$$\begin{aligned} i\Delta^{(-)}(x; x') &= \langle \Omega | \hat{\phi}(x') \hat{\phi}(x) | \Omega \rangle = \int \frac{d^{D-1}k}{(2\pi)^{D-1}} e^{i\vec{k}_\perp \cdot \Delta\vec{x}_\perp + \frac{i}{2}\Omega_+(\vec{k})\Delta v} \phi_-(u, \vec{k}) \phi_+(u', -\vec{k}) \\ &= \int \frac{d^{D-1}k}{(2\pi)^{D-1}} e^{-i\vec{k}_\perp \cdot \Delta\vec{x}_\perp + \frac{i}{2}\Omega_-(\vec{k})\Delta v} \phi_-(u, -\vec{k}) \phi_+(u', \vec{k}), \end{aligned} \quad (5.2)$$

where $\Delta\vec{x}_\perp = \vec{x}_\perp - \vec{x}'_\perp$, $\Delta v = v - v'$, and $\phi_+(u, \vec{k})$ and $\phi_-(u', \vec{k})$ are the positive and negative frequency mode functions obeying,

$$\left(\partial_u \pm \frac{i}{2\Omega_\mp} \left[(g^{ij}(u) - \delta_\perp^{ij}) k_i k_j \right] \pm \frac{i}{2} \Omega_\pm \right) [\gamma^{1/4}(u) \phi_\pm(u, \vec{k})] = 0, \quad (5.3)$$

where $\Omega_\pm(\vec{k}) = \omega \pm k^{D-1}$, $\gamma(u) = \det[g_{ij}(u)]$, and $\omega = \sqrt{\|\vec{k}\|^2 + m^2}$. This is a first order differential equation in u and therefore can be easily solved. The properly normalized, ground state solution of Eq. (5.3) is given by,

$$\phi_\pm(u, \vec{k}) = \frac{1}{\gamma^{1/4}(u)} \sqrt{\frac{\hbar}{2\omega}} \exp \left[\mp \frac{i\Omega_\pm}{2} \left(u + \frac{k_i k_j}{\omega_\pm^2} \int^u d\bar{u} (g^{ij}(\bar{u}) - \delta^{ij}) \right) \right], \quad (5.4)$$

where $\omega_\pm^2 = \omega^2 - (k^{D-1})^2$. The Wightman functions (5.1–5.2) satisfy, $i\Delta^{(-)}(x'; x) = i\Delta^{(+)}(x; x')$ and $i\Delta^{(-)}(x; x') = [i\Delta^{(+)}(x; x')]^*$. The integrals in Eqs. (5.1) and (5.2) can be performed by the methods explicated in Appendices A and B or Ref. [1] resulting in the Wightman functions in Eq. (2.4).

Appendix B: Inverse quartic root cuts

In the case of polarized gravitational waves, the cut structure in the complex plane may be richer than the one shown in figure 1. To see that, let us analyse the term $1/[\gamma(u)\gamma(u')]^{1/4}$ in Eq. (3.25) in the complex Δu -plane. For simplicity we consider here maximally polarized gravitational waves. Let us begin with the + polarization. Recalling that $u = U + \Delta u/2$ and $u' = U - \Delta u/2$ one can write,

$$\gamma(u) = 1 - h_+^2 \cos^2(\omega_g u) = 1 - \frac{h_+^2}{2} \left[1 + \cos(2\omega_g U) \cos(\omega_g \Delta u) - \sin(2\omega_g U) \sin(\omega_g \Delta u) \right],$$

from which we infer,

$$\gamma(u)\gamma(u') = 1 - h_+^2 \left[1 + \cos(2\omega_g U) \cos(\omega_g \Delta u) \right] + \frac{h_+^4}{4} \left[\left(1 + \cos(2\omega_g U) \cos(\omega_g \Delta u) \right)^2 - \sin^2(2\omega_g U) \sin^2(\omega_g \Delta u) \right].$$

To see that there are poles in the complex Δu plane, let us transform this equation into the variables, $\omega_g \Delta u \rightarrow 2i\theta - 2\zeta$,

$$\cosh^2(2\theta + 2i\zeta) - 2 \left(\frac{2}{h_+^2} - 1 \right) \cos(2\omega_g U) \cosh(2\theta + 2i\zeta) + \left(\frac{4}{h_+^4} - \frac{4}{h_+^2} + \cos(2\omega_g U) \right) = 0. \quad (5.5)$$

The roots of this quadratic equation are given by,

$$[\cosh(2\theta + 2i\zeta)]_\pm = \left(\frac{2}{h_+^2} - 1 \right) \cos(2\omega_g U) \pm i \frac{2}{h_+} \sqrt{\frac{1}{h_+^2} - 1} \sin(2\omega_g U), \quad (5.6)$$

or equivalently,

$$\begin{aligned} \cosh(2\theta) &= \frac{2}{h_+^2} - 1 \implies \theta_\pm = \frac{1}{2} \ln \left[\frac{2}{h_+^2} - 1 \pm \frac{2}{h_+} \sqrt{\frac{1}{h_+^2} - 1} \right] = \pm \frac{1}{2} \ln \left[\frac{2}{h_+^2} - 1 + \frac{2}{h_+} \sqrt{\frac{1}{h_+^2} - 1} \right], \\ \zeta_\pm &= \pm \omega_g U. \end{aligned} \quad (5.7)$$

The poles in the case of a \times -polarized wave are given by simply replacing $h_+ \rightarrow h_\times$. The result in Eq. (5.7) shows that polarized gravitational waves generate a richer structure of cuts in the complex Δu plane. In particular, the term $1/[\gamma(u)\gamma(u')]^{1/4}$ generates four of its own inverse quartic root cuts, whose real parts ‘walk’ along the real axis as, $\Re[\Delta u] = \pm 2U$, and the cuts begin at, $\Im[\Delta u] = \theta_\pm/\omega_g$. In this work we not attempt to model the detector transition rate due to these cuts.

References

- [1] R. van Haasteren and T. Prokopec, “Scalar propagator for planar gravitational waves,” [arXiv:2204.12930 [gr-qc]].
- [2] J. Garriga and E. Verdaguer, “Scattering of quantum particles by gravitational plane waves,” Phys. Rev. D **43** (1991), 391-401 doi:10.1103/PhysRevD.43.391
- [3] P. Jones, P. McDougall and D. Singleton, “Particle production in a gravitational wave background,” Phys. Rev. D **95** (2017) no.6, 065010 doi:10.1103/PhysRevD.95.065010 [arXiv:1610.02973 [gr-qc]].
- [4] P. Jones, P. McDougall, M. Ragsdale and D. Singleton, “Scalar field vacuum expectation value induced by gravitational wave background,” Phys. Lett. B **781** (2018), 621-625 doi:10.1016/j.physletb.2018.04.055 [arXiv:1706.09402 [gr-qc]].
- [5] P. M. Zhang, C. Duval, G. W. Gibbons and P. A. Horvathy, “The Memory Effect for Plane Gravitational Waves,” Phys. Lett. B **772** (2017), 743-746 doi:10.1016/j.physletb.2017.07.050 [arXiv:1704.05997 [gr-qc]].
- [6] P. M. Zhang, C. Duval, G. W. Gibbons and P. A. Horvathy, “Velocity Memory Effect for Polarized Gravitational Waves,” JCAP **05** (2018), 030 doi:10.1088/1475-7516/2018/05/030 [arXiv:1802.09061 [gr-qc]].
- [7] M. Siddhartha and A. Dasgupta, “Scalar and fermion field interactions with a gravitational wave,” Class. Quant. Grav. **37** (2020) no.10, 105001 doi:10.1088/1361-6382/ab79d6 [arXiv:1907.07531 [gr-qc]].
- [8] Q. Xu, S. A. Ahmad and A. R. H. Smith, “Gravitational waves affect vacuum entanglement,” Phys. Rev. D **102** (2020) no.6, 065019 doi:10.1103/PhysRevD.102.065019 [arXiv:2006.11301 [quant-ph]].
- [9] B. H. Chen and D. W. Chiou, “Response of the Unruh-DeWitt detector in a gravitational wave background,” Phys. Rev. D **105** (2022) no.2, 024053 doi:10.1103/PhysRevD.105.024053 [arXiv:2109.14183 [gr-qc]].
- [10] W. G. Unruh, “Notes on black hole evaporation,” Phys. Rev. D **14** (1976), 870 doi:10.1103/PhysRevD.14.870
- [11] B. S. DeWitt in S. W. Hawking and W. Israel, “General Relativity: An Einstein Centenary Survey,”
- [12] N. D. Birrell and P. C. W. Davies, “Quantum Fields in Curved Space,” doi:10.1017/CBO9780511622632
- [13] A. Bourgoin, C. L. Poncin-Lafitte, S. Mathis and M. C. Angonin, “Impact of dipolar magnetic fields on gravitational wave strain by galactic binaries,” [arXiv:2201.03226 [gr-qc]].
- [14] P. Amaro-Seoane, J. Andrews, M. A. Sedda, A. Askar, R. Balasov, I. Bartos, S. S. Bavera, J. Bellovary, C. P. L. Berry and E. Berti, *et al.* “Astrophysics with the Laser Interferometer Space Antenna,” [arXiv:2203.06016 [gr-qc]].